Cooperative Aerial Transportation without Communication: the Role of Internal Force for Pose Regulation

Marco Tognon, Chiara Gabellieri, Lucia Pallottino, Antonio Franchi

Cooperative Aerial Transportation without Communication: the Role of Internal Force for Pose Regulation

Marco Tognon[1], Chiara Gabellieri[1†], Lucia Pallottino[2], and Antonio Franchi[1]

***Abstract*— This paper considers the study of cooperative transportation of a cable-suspended load with two aerial robots and without explicit communication. The role of the internal force for the asymptotic stability of the beam-position/beam-attitude equilibria is analyzed in depth and explained thoroughly. Using a nonlinear Lyapunov-based approach, we prove that that if a non-zero internal force is chosen then asymptotic stabilization of any desired beam-position/beam-attitude configuration can be achieved by using a decentralized and communication-less master-slave admittance controller. If, conversely, a zero internal force is chosen, as done in the majority of the state-of-the-art algorithms, the attitude of the beam is not controllable without communication. Non-zero internal force can be interpreted then as a fundamental factor that enables the use of cables as implicit communication means between the two aerial vehicles in replacement of the explicit ones. The theoretical findings are validated through numerical simulations with added noise and realistic uncertainty.**

I. Introduction

Over the last decade UAVs (Unmanned Aerial Vehicles) have risen the interest of a larger and larger audience for their wide application domain. Recently, aerial physical interaction, using aerial manipulators [1] or exploiting physical links as cables [2], has become a very popular topic. One very interesting and applicative problem is the manipulation of an object. For this task, UAVs are very suited but usually small and characterized by a limited payload capacity [3], [4]. A cooperative approach allows to lift larger and heavier loads, providing a safer and less expensive solution w.r.t. the deployment of a single but more powerful aerial robot.

Many works have targeted the problem of cooperative load manipulation, proposing different methods and solutions. In [5], [6] cooperative aerial transportation of a rigid and elastic object is considered, respectively. In [7]–[9] the same problem is addressed using aerial vehicles with a robotic arm. Aerial manipulation via cables is a particularly interesting solution to the problem since it permits to reduce the couplings between load and the robot attitude dynamics. Examples of cooperative aerial manipulation using cables are studied in [10]–[13]. All these examples rely on a centralized and model-based control strategies. However, a decentralized algorithm, as the one in [14], is more scalable w.r.t. the number of robots and more robust to the failure of an agent. Another example, in [15] the possibility of using a swarm of UAVs to grasp an object as a flying hand is discussed.

Explicit communication in decentralized algorithms is the major bottle-neck. Communication delays and packet loss can affect the performances but even the stability of the controlled systems. Limiting the need for explicit communication allows to reduce the complexity and to make the algorithm more scalable. In [16] the authors proposed one of the first decentralized leader-follower algorithm without explicit communication, for objects transportation performed by mobile ground robots. The problem of transportation of a cable suspended beam-like load by two aerial robots has been addressed in [17]. Here a master-slave (i.e, leader-follower) paradigm without explicit communication is exploited. In particular, the horizontal position of the slave robot is controlled with an admittance filter, trying to keep the cable always vertical (zero internal force). A similar approach has been proposed in [18] but relying on a visual feedback. However, those methods do not deal with the load pose control and do not provide formal stability proofs.

For the same system, we propose a decentralized algorithm relying only on implicit communication. Our algorithm uses a master-slave architecture, where both robots are controlled with an admittance filter, to make the master and the overall system more compliant to external disturbances. One of main contributions of our paper is the constructive and intuitive method to chose the controller input to stabilize the load in a desired pose (both position and orientation), provided that the load parameters are known. We show that those constant input are parametrized by the internal force of the load. A formal characterization of the equilibria and the relative stability, given a certain desired internal force, is provided.

The paper is organized as follows. In Sec. II we derive the model. In Sec. III we present the control strategy, the equilibria and stability analysis. Simulation results and conclusive discussions are presented in Sec. IV and V, respectively.

II. Modeling

The considered system and its major variables are shown in Fig. 1. The beam-like *load* to be manipulated is modeled as a rigid body with mass $m_L \in \mathbb{R}_{>0}$ and a positive definite inertia matrix $\boldsymbol{J}_L \in \mathbb{R}^{3\times3}$. We define the frame $\mathscr{F}_L = \{O_L, \boldsymbol{x}_L, \boldsymbol{y}_L, \boldsymbol{z}_L\}$ rigidly attached to the load, where O_L is the the load center of mass (CoM). Furthermore, we define an inertial frame $\mathscr{F}_W = \{O_W, \boldsymbol{x}_W, \boldsymbol{y}_W, \boldsymbol{z}_W\}$ with $\boldsymbol{z}_W$ oriented in the opposite direction of the gravity vector. The configuration of the load is then described by the position and orientationof

[†]The first two authors have equally collaborated to the manuscript, and can both considered as first author.

[1]LAAS-CNRS, Université de Toulouse, CNRS, Toulouse, France, antonio.franchi@laas.fr, mtognon@laas.fr, cgabellieri@laas.fr

[2]Centro di ricerca E. Piaggio, Università di Pisa, Largo Lucio Lazzarino 1, 56122,Pisa, Italy lucia.pallottino@unipi.it

This work has been funded by the European Union's Horizon 2020 research and innovation program under grant agreement No 644271 AEROARMS.

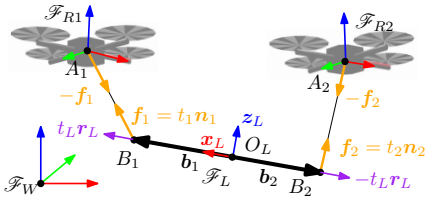

Fig. 1: Representation of the system and its major variables. For the frame axes, the RGB convention is used, where the red, green, and blues arrow represent the x, y, and z axes of the frame respectively.

$\mathscr{F}_L$ with respect to $\mathscr{F}_W$, i.e., by the vector[1] ${}^W\boldsymbol{p}_L \in \mathbb{R}^3$ and the rotation matrix ${}^W\boldsymbol{R}_L \in SO(3)$, respectively. Its dynamics is given by the Newton-Euler equations

$$\begin{aligned} m_L\ddot{\boldsymbol{p}}_L &= -m_L g\boldsymbol{e}_3 + \boldsymbol{f}_e \\ \dot{\boldsymbol{R}}_L &= \boldsymbol{S}(\boldsymbol{\omega}_L)\boldsymbol{R}_L \\ \boldsymbol{J}_L\dot{\boldsymbol{\omega}}_L &= -\boldsymbol{S}(\boldsymbol{\omega}_L)\boldsymbol{J}_L\boldsymbol{\omega}_L + \boldsymbol{\tau}_e - \boldsymbol{\omega}_L^T\boldsymbol{B}_L\boldsymbol{\omega}_L, \end{aligned}$$

where, $\boldsymbol{\omega}_L \in \mathbb{R}^3$ is the angular velocity of $\mathscr{F}_L$ w.r.t. $\mathscr{F}_W$ expressed in $\mathscr{F}_L$, $\boldsymbol{S}(\star)$ is the operator such that $\boldsymbol{S}(\boldsymbol{x})\boldsymbol{y} = \boldsymbol{x}\times\boldsymbol{y}$, g is the gravitational constant, $\boldsymbol{e}_i$ is the canonical unit vector with a 1 in the i-th entry, $\boldsymbol{f}_e$ and $\boldsymbol{\tau}_e \in \mathbb{R}^3$ are the sum of external forces and moments acting on the load, respectively, and the positive definite matrix $\boldsymbol{B}_L \in \mathbb{R}^{3\times3}$ is a damping factor modeling the energy dissipation phenomena.

The load is transported by two aerial robots by means of two cables, one for each robot. We denote with A_i the attachment point of the i-th cable to the i-th robot, with $i = 1,2$, and we define the frame $\mathscr{F}_{Ri} = \{A_i, \boldsymbol{x}_{Ri}, \boldsymbol{y}_{Ri}, \boldsymbol{z}_{Ri}\}$ rigidly attached to the robot and centered in the attachment point. The i-th robot configuration is described by the position and orientation of $\mathscr{F}_{Ri}$ with respect to $\mathscr{F}_W$, denoted by the vector $\boldsymbol{p}_{Ri} \in \mathbb{R}^3$, and the rotation matrix $\boldsymbol{R}_{Ri} \in SO(3)$, respectively. We assume that the aerial robot can track any C^2 trajectory with negligible error in the domain of interest, independently from external disturbances. Indeed, with the recent robust controllers and disturbance observers for aerial vehicles, one can obtain very precise motions, even in the presence of external disturbances. Moreover, if the used robot has a multi-directional thrust, as, e.g., the one presented in [19], then this assumption is exactly met thanks to its ability to compensate any external force almost instantaneously. The closed loop translational dynamics of the robot subject to the position controller is then assumed as the one of a double integrator: $\ddot{\boldsymbol{p}}_{Ri} = \boldsymbol{u}_{Ri}$, where $\boldsymbol{u}_{Ri}$ is a virtual input to be designed. At this stage it might seem that we are assuming a controller and an actuation system that can make the platform 'infinitely stiff' w.r.t. the force produced by the cable. However, as it will be clear in the following, this is not true in practice. In fact, we shall re-introduce a compliant behavior by suitably designing the input $\boldsymbol{u}_{Ri}$ to adapt to the force produced by the cable on the robot. This is a common paradigm in interaction control.

The other end of the i-th cable is attached to the load at the anchoring point B_i described by the vector ${}^L\boldsymbol{b}_i \in \mathbb{R}^3$ denoting its position with respect to $\mathscr{F}_L$. The position of B_i in $\mathscr{F}_W$ is then expressed by $\boldsymbol{b}_i = \boldsymbol{p}_L + \boldsymbol{R}_L\,{}^L\boldsymbol{b}_i$.

Assumption 1. The two anchoring points are placed such that the load CoM coincides with their middle point, i.e., ${}^L\boldsymbol{b}_1 = -{}^L\boldsymbol{b}_2$. This assumption is rather easy to meet in practice, even for a load with non uniformly distributed mass.

In order to simplify the following discussion we assume, without loss of generality, that $\boldsymbol{x}_L$ is aligned with the line passing through the two anchoring points and pointing toward the first one. By doing so it results ${}^L\boldsymbol{b}_1 = [\|{}^L\boldsymbol{b}_1\|\,0\,0]^T$.

Cable-to-robot and cable-to-load connections are done in such a way that no rotational constraints are present. Hence, we can model them as passive and massless rotational joints.

We model the i-th cable as a unilateral spring along its principal direction, characterized by a constant elastic coefficient $k_i \in \mathbb{R}_{>0}$, a constant nominal length denoted by l_{0i} and a negligible mass and inertia w.r.t. the ones of the robots and of the load. The attitude of the cable is described by the normalized vector, $\boldsymbol{n}_i = \boldsymbol{l}_i/\|\boldsymbol{l}_i\|$, where $\boldsymbol{l}_i = \boldsymbol{p}_{Ri} - \boldsymbol{b}_i$. Given a certain elongation $\|\boldsymbol{l}_i\|$ of the cable, the latter produces a force acting on the load at B_i equal to:

$$\boldsymbol{f}_i = t_i\boldsymbol{n}_i \quad \text{where} \quad t_i = \begin{cases} k_i(\|\boldsymbol{l}_i\| - l_{0i}) & \text{if } \|\boldsymbol{l}_i\| - l_{0i} > 0 \\ 0 & \text{otherwise} \end{cases}, \tag{1}$$

$t_i \in \mathbb{R}_{\geq 0}$ denotes the tension along the cable and it is given by the simplified Hooke's law. When the tension is zero the cable is considered slack. However, as usually done in the related literature, we assume that the controller and the gravity force always maintain the cables taut, at least in the domain of interest.[2] The force produced at the other hand of the cable, namely on the i-th robot at A_i, is equal to $-\boldsymbol{f}_i$.

Considering the forces that robots and load exchange by means of the cables, the dynamics of the full system is:

$$\begin{aligned} \dot{\boldsymbol{v}}_R &= \boldsymbol{u}_R \\ \dot{\boldsymbol{v}}_L &= \boldsymbol{M}_L^{-1}\left(-\boldsymbol{c}_L(\boldsymbol{q}_L) - \boldsymbol{g}_L + \boldsymbol{G}(\boldsymbol{q}_L)\boldsymbol{f}\right), \end{aligned} \tag{2}$$

where $\boldsymbol{q}_R = [\boldsymbol{p}_{R1}^T\ \boldsymbol{p}_{R2}^T]^T$, $\boldsymbol{q}_L = (\boldsymbol{p}_L, \boldsymbol{R}_L)$, $\boldsymbol{v}_R = [\dot{\boldsymbol{p}}_{R1}^T\ \dot{\boldsymbol{p}}_{R2}^T]^T$, $\boldsymbol{v}_L = [\dot{\boldsymbol{p}}_L^T\ \boldsymbol{\omega}_L^T]^T$, $\boldsymbol{u}_R = [\boldsymbol{u}_{R1}^T\ \boldsymbol{u}_{R2}^T]^T$, $\boldsymbol{f} = [\boldsymbol{f}_1^T\ \boldsymbol{f}_2^T]^T$, $\boldsymbol{M}_L = \mathrm{diag}\,(m_L\boldsymbol{I}_3, \boldsymbol{J}_L)$, $\boldsymbol{g}_L = [-m_L g\boldsymbol{e}_3^T\ \boldsymbol{0}]^T$ and

$$\boldsymbol{c}_L = \begin{bmatrix} \boldsymbol{0} \\ \boldsymbol{S}(\boldsymbol{\omega}_L)\boldsymbol{J}_L\boldsymbol{\omega}_L \end{bmatrix} \qquad \boldsymbol{G} = \begin{bmatrix} \boldsymbol{I}_3 & \boldsymbol{I}_3 \\ \boldsymbol{S}({}^L\boldsymbol{b}_1)\boldsymbol{R}_L^T & \boldsymbol{S}({}^L\boldsymbol{b}_2)\boldsymbol{R}_L^T \end{bmatrix}.$$

Control problem

In this work we aim to: 1) stabilize the load at a desired configuration, $\bar{\boldsymbol{q}}_L = (\bar{\boldsymbol{p}}_L, \bar{\boldsymbol{R}}_L)$; 2) preserve the stability of the load during its transportation.

Assuming a perfect knowledge of the dynamic model of the system, and a perfect state estimation, one could use a centralized control approach as the ones in [10], [11]. Those methods are heavily model based, hence are not robust to model uncertainties. We shall instead provide a method that preserve the stability even with an inaccurate model. Furthermore, we are interested in solving the mentioned

[1] The left superscript indicates the reference frame. From now on, $\mathscr{F}_W$ is considered as reference frame when the superscript is omitted.

[2] We are not interested here in 'fancy' acrobatic motions of the load but rather on designing a decentralized and communicationless control law that can be employed in realistic scenarios.

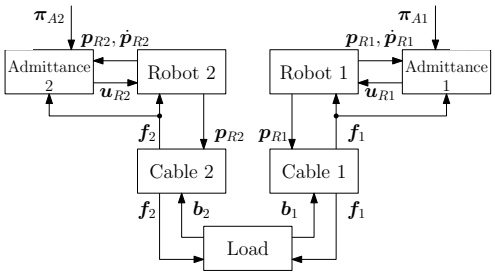

Fig. 2: Schematic representation of the overall system including both physical and control blocks.

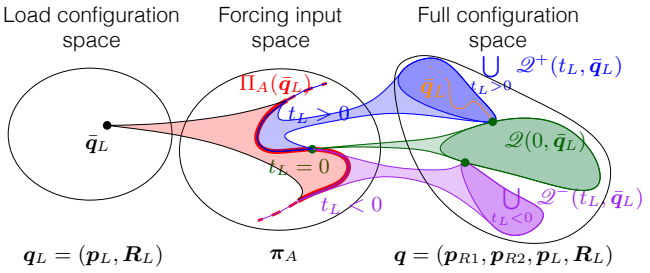

Fig. 3: Relation between the equilibria and forcing control input. The relations between the left and middle sets and the one between the middle and right sets represent equilibria direct and inverse problems, respectively.

objectives using a decentralized approach without explicit communication between the robots and relying on a minimal sensorial setup.

III. Control Design and Equilibria

To achieve the control objectives of Sec. II we propose the use of an admittance filter for *both* robots, i.e., setting:

$$\boldsymbol{u}_{Ri} = \boldsymbol{M}_{Ai}^{-1}\left(-\boldsymbol{B}_{Ai}\dot{\boldsymbol{p}}_{Ri} - \boldsymbol{K}_{Ai}\boldsymbol{p}_{Ri} - \boldsymbol{f}_i + \boldsymbol{\pi}_{Ai}\right), \tag{3}$$

where the tree positive definite matrices $\boldsymbol{M}_{Ai}, \boldsymbol{B}_{Ai}, \boldsymbol{K}_{Ai} \in \mathbb{R}^{3\times 3}$ are the virtual inertia of the robot, the virtual damping, and the stiffness of a virtual spring attached to the robot, and $\boldsymbol{\pi}_{Ai} \in \mathbb{R}^3$ is an additional input parameter. Notice that (3) requires only local information, i.e., the local state of the robot $(\boldsymbol{p}_{Ri}, \dot{\boldsymbol{p}}_{Ri})$, and the force applied by the cable $\boldsymbol{f}_i$. The first can be retrieved with standard on-board sensors for aerial vehicles, while the second can be directly measured by an on-board force sensor or estimated by a model-based observer as done in [17], [19]. Therefore, the control method is decentraized and does not require explicit communication. Indeed each robot uses only local measurement without the need of direct communication with the other agent. A schematic representation of the overall control strategy is shown in Fig. 2.

Combining equations (2) and (3) we can write the closed loop system dynamics as

$$\dot{\boldsymbol{v}} = m(\boldsymbol{q}, \boldsymbol{v}, \boldsymbol{\pi}_A) = \begin{bmatrix} \boldsymbol{M}_A^{-1}(-\boldsymbol{B}_A\dot{\boldsymbol{p}}_R - \boldsymbol{K}_A\boldsymbol{p}_R - \boldsymbol{f} + \boldsymbol{\pi}_A) \\ \boldsymbol{M}_L^{-1}(-\boldsymbol{c}_L(\boldsymbol{v}_L) - \boldsymbol{g}_L + \boldsymbol{G}\boldsymbol{f}) \end{bmatrix} \tag{4}$$

with $\boldsymbol{q} = (\boldsymbol{q}_R, \boldsymbol{q}_L)$, $\boldsymbol{v} = [\boldsymbol{v}_R^T \ \boldsymbol{v}_L^T]^T$, $\boldsymbol{\pi}_A = [\boldsymbol{\pi}_{A1}^T \ \boldsymbol{\pi}_{A2}^T]^T$, and $\boldsymbol{f} = [\boldsymbol{f}_1^T \ \boldsymbol{f}_2^T]^T$ where $\boldsymbol{f}_i$ is given in (1), and is a function of the state. Furthermore $\boldsymbol{M}_A = \mathrm{diag}(\boldsymbol{M}_{A1}, \boldsymbol{M}_{A2})$, $\boldsymbol{B}_A = \mathrm{diag}(\boldsymbol{B}_{A1}, \boldsymbol{B}_{A2})$ and $\boldsymbol{K}_A = \mathrm{diag}(\boldsymbol{K}_{A1}, \boldsymbol{K}_{A2})$.

In order to coordinate the motions of the robots in a decentralized way we propose a master-slave approach. In this way only one robot, namely the designated master, will have an active control of the system. On the other hand, the slave will passively follow the master partially compensating the weight of the load and contributing to preserve the stability of the system. Choosing robot 1 as master and robot 2 as slave we simply set $\boldsymbol{K}_{A1} \neq \boldsymbol{0}$, $\boldsymbol{K}_{A2} = \boldsymbol{0}$ to obtain the sought master-slave paradigm.

We say that $\boldsymbol{q}$ is an *equilibrium configuration* if $\exists\ \boldsymbol{\pi}_A$ s.t.

$$\boldsymbol{0} = m(\boldsymbol{q}, \boldsymbol{0}, \boldsymbol{\pi}_A), \tag{5}$$

i.e, if the corresponding zero-velocity state $(\boldsymbol{q}, \boldsymbol{0})$ is a forced equilibrium for the system (4) for a certain forcing input $\boldsymbol{\pi}_A$. We say that an equilibrium configuration $\boldsymbol{q}$ is stable, unstable, or asymptotically stable if $(\boldsymbol{q}, \boldsymbol{0})$ is stable, unstable, or asymptotically stable, respectively.

In the following parts of this Section we shall prove that for any desired load configuration $\bar{\boldsymbol{q}}_L$ there exists a set $\Pi_A(\bar{\boldsymbol{q}}_L) \subset \mathbb{R}^6$ such that for any $\boldsymbol{\pi}_A \in \Pi_A(\bar{\boldsymbol{q}}_L)$ one can compute a $\bar{\boldsymbol{q}}_R$, depending $\bar{\boldsymbol{q}}_L$ and $\boldsymbol{\pi}_A$, that makes $\bar{\boldsymbol{q}} = [\bar{\boldsymbol{q}}_L^T \ \bar{\boldsymbol{q}}_R^T]^T$ an asymptotically stable equilibrium with $\boldsymbol{\pi}_A$ as forcing input. Furthermore, we shall also give the analytic expression of $\Pi_A(\bar{\boldsymbol{q}}_L)$ and the fundamental guidelines on how to choose $\boldsymbol{\pi}_A \in \Pi_A(\bar{\boldsymbol{q}}_L)$.

As we shall see, a key role in all the following analyses is played by the *load internal force*, defined as

$$t_L := \tfrac{1}{2}\boldsymbol{f}^T \begin{bmatrix} \boldsymbol{I}_3 & -\boldsymbol{I}_3 \end{bmatrix}^T \boldsymbol{R}_L \boldsymbol{e}_1 =: \tfrac{1}{2}\boldsymbol{f}^T \boldsymbol{r}_L. \tag{6}$$

For the particular choice of $\boldsymbol{r}_L$, we have that if $t_L > 0$ the internal force is a *tension* (the work of the internal force is positive if the distance between the anchoring points increases) while if $t_L < 0$ the internal force is a *compression* (viceversa, the work is positive if the distance decreases).

A. Equilibrium Configurations of the Closed Loop System

We firstly carefully analyze and characterize the relation between equilibrium configurations, from now on simply called *equilibria*, and the forcing input $\boldsymbol{\pi}_A$. In particular, in the following we study:

- which is the *set of inputs* (and corresponding robot positions) that equilibrates a desired $\bar{\boldsymbol{q}}_L$ (theorem 1);
- which is the *set of equilibria* if the particular input chosen in the aforementioned set is applied on the system (theorem 2).

These two problems are referred to as the *equilibria direct problem* and *equilibria inverse problem*, respectively. A schematic representation of the results described in the theorems is given in Fig. 3.

Theorem 1 (equilibria direct problem)**.** *Consider the closed loop system* (4) *and assume that the load is at a given desired configuration* $\boldsymbol{q}_L = \bar{\boldsymbol{q}}_L = (\bar{\boldsymbol{p}}_L, \bar{\boldsymbol{R}}_L)$*. For each internal force* $t_L \in \mathbb{R}$*, there exists a unique constant value for the forcing input* $\boldsymbol{\pi}_A = \bar{\boldsymbol{\pi}}_A$ *(and a unique position of the robots* $\boldsymbol{q}_R = \bar{\boldsymbol{q}}_R$*) such that* $\bar{\boldsymbol{q}} = (\bar{\boldsymbol{q}}_L, \bar{\boldsymbol{q}}_R)$ *is an equilibrium of the system.*

In particular $\bar{\boldsymbol{\pi}}_A$ *and* $\bar{\boldsymbol{q}}_R = [\bar{\boldsymbol{p}}_{R1}^T \; \bar{\boldsymbol{p}}_{R2}^T]^T$ *are given by*

$$\bar{\boldsymbol{\pi}}_A(\bar{\boldsymbol{q}}_L, t_L) = \boldsymbol{K}_A \bar{\boldsymbol{q}}_R + \bar{\boldsymbol{f}} \tag{7}$$

$$\bar{\boldsymbol{p}}_{Ri}(\bar{\boldsymbol{q}}_L, t_L) = \bar{\boldsymbol{p}}_L + \bar{\boldsymbol{R}}_L {}^L\boldsymbol{b}_i + \left(\frac{\|\bar{\boldsymbol{f}}_i\|}{k_i} + l_{0i} \right) \frac{\bar{\boldsymbol{f}}_i}{\|\bar{\boldsymbol{f}}_i\|}, \;\; i = 1, 2, \tag{8}$$

where

$$\bar{\boldsymbol{f}}(\bar{\boldsymbol{q}}_L, t_L) = \begin{bmatrix} \bar{\boldsymbol{f}}_1 \\ \bar{\boldsymbol{f}}_2 \end{bmatrix} = \frac{m_L g}{2} \begin{bmatrix} \boldsymbol{I}_3 \\ \boldsymbol{I}_3 \end{bmatrix} \boldsymbol{e}_3 + t_L \begin{bmatrix} \boldsymbol{I}_3 \\ -\boldsymbol{I}_3 \end{bmatrix} \bar{\boldsymbol{R}}_L \boldsymbol{e}_1. \tag{9}$$

Proof. The desired load configuration $\bar{\boldsymbol{q}}_L$ can be equilibrated if it exists at least a $\bar{\boldsymbol{q}}_R$ and a $\boldsymbol{\pi}_A$ such that:

$$m(\bar{\boldsymbol{q}}, \boldsymbol{0}, \boldsymbol{\pi}_A, \boldsymbol{0}) = \boldsymbol{0}. \tag{10}$$

Consider the last six rows of (10). We must find the $\boldsymbol{f}$ resolving

$$\boldsymbol{G}\boldsymbol{f} = \boldsymbol{g}_L. \tag{11}$$

$\boldsymbol{G}$ is not invertible since $\text{rank}(\boldsymbol{G}) = 5$, therefore we have to verify that a solution for (11) exists. Expanding (11) we obtain

$$\boldsymbol{f}_1 + \boldsymbol{f}_2 = -m_L g \boldsymbol{e}_3 \tag{12}$$

$$\boldsymbol{S}({}^L\boldsymbol{b}_1)\bar{\boldsymbol{R}}_L^T \boldsymbol{f}_1 + \boldsymbol{S}({}^L\boldsymbol{b}_2)\bar{\boldsymbol{R}}_L^T \boldsymbol{f}_2 = \boldsymbol{0}. \tag{13}$$

Then, substituting in (13) the $\boldsymbol{f}_1$ obtained from (12) we have

$$2\boldsymbol{S}({}^L\boldsymbol{b}_1)\bar{\boldsymbol{R}}_L^T \boldsymbol{f}_2 = -\boldsymbol{S}({}^L\boldsymbol{b}_1)\bar{\boldsymbol{R}}_L^T m_L g \boldsymbol{e}_3, \tag{14}$$

which has always at least the solution $\boldsymbol{f}_2 = m_L g \boldsymbol{e}_3/2$. Therefore, all the solutions of (11) can be written as

$$\bar{\boldsymbol{f}} = \boldsymbol{G}^\dagger \boldsymbol{g}_L + \boldsymbol{r}_L t_L, \tag{15}$$

where $\boldsymbol{G}^\dagger = 1/2[\boldsymbol{I}_3 \; \boldsymbol{I}_3]^T$ is the pseudo inverse of $\boldsymbol{G}$, $\boldsymbol{r}_L \in \mathbb{R}^6$ is a vector in $\ker(\boldsymbol{G})$, and $t_L \in \mathbb{R}$ is any value. We computed $\boldsymbol{r}_L$ from (12) and (13) putting the right hand side equal to zero, obtaining after some algebra $\boldsymbol{r}_L = \begin{bmatrix} \boldsymbol{I}_3 & -\boldsymbol{I}_3 \end{bmatrix}^T \bar{\boldsymbol{R}}_L \boldsymbol{e}_1$, as in the definition (6). Therefore, equation (15) can be rewritten as (9). The expression of $\bar{\boldsymbol{p}}_{Ri}$ in (8) is computed using (1) and the kinematics of the system. Notice that (8) is singular when $\bar{\boldsymbol{f}}_i = \boldsymbol{0}$ for some i. However this can always be avoided properly choosing t_L.

Lastly, from the first six rows of (10) we have that $\bar{\boldsymbol{q}}_L$ is equilibrated if $\boldsymbol{\pi}_A = \bar{\boldsymbol{\pi}}_A$, where $\bar{\boldsymbol{\pi}}_A$ is defined as in (7). □

Remark 1. Based on Theorem 1 we can define a set $\Pi_A(\bar{\boldsymbol{q}}_L) = \{\boldsymbol{\pi}_A \in \mathbb{R}^6 : \boldsymbol{\pi}_A = \bar{\boldsymbol{\pi}}_A(\bar{\boldsymbol{q}}_L, t_L) \text{ for } t_L \in \mathbb{R}\}$ which has dimension 1, since it is parametrized by the scalar $t_L \in \mathbb{R}$. This set is depicted as a curve in the middle set of Fig. 3.

Remark 2. The expression (9) of the cable forces that equilibrate the system is split in two parts. The first, i.e., $\boldsymbol{G}^\dagger \boldsymbol{g}_L$, compensates the gravity force and the second generates internal forces that, for the system under consideration, are always along the direction $(\boldsymbol{b}_1 - \boldsymbol{b}_2)$.

Remark 3. Theorem 1 and its constructive proofs, give an intuitive method for choosing the forcing input $\boldsymbol{\pi}_A$ given a desired load configuration $\bar{\boldsymbol{q}}_L$ to equilibrate. In particular one has only to choose the value of the internal force t_L. We shall show that is always preferable to choose $t_L > 0$ to obtain an asymptotically stable equilibrium.

Once t_L is chosen and the input $\boldsymbol{\pi}_A = \bar{\boldsymbol{\pi}}_A(t_L, \bar{\boldsymbol{q}}_L)$ is applied to the system, it is not in general granted that $(\bar{\boldsymbol{q}}_L, \bar{\boldsymbol{q}}_R)$ is the only equilibrium of the closed loop system (4). The following results will show how many other equilibria exist and which is their nature.

Theorem 2 (equilibria inverse problem)**.** *Given* $t_L \in \mathbb{R}$ *and the corresponding* $\bar{\boldsymbol{\pi}}_A \in \Pi_A(\bar{\boldsymbol{q}}_L)$ *computed as in* (7)*, the equilibria of the system* (4)*, when the input* $\boldsymbol{\pi}_A = \bar{\boldsymbol{\pi}}_A(t_L, \bar{\boldsymbol{q}}_L)$ *is applied, are all and only the ones described by the following conditions*

$$\begin{aligned} t_L \boldsymbol{R}_L \boldsymbol{e}_1 \times \bar{\boldsymbol{R}}_L \boldsymbol{e}_1 &= \boldsymbol{0} \\ \boldsymbol{p}_{R1} &= \bar{\boldsymbol{p}}_{R1} \\ \boldsymbol{p}_L = \boldsymbol{p}_{R1} - \boldsymbol{R}_L {}^L\boldsymbol{b}_1 - \left(\frac{\|\bar{\boldsymbol{f}}_1\|}{k_1} + l_{01} \right) \frac{\bar{\boldsymbol{f}}_1}{\|\bar{\boldsymbol{f}}_1\|} &= \\ = \bar{\boldsymbol{p}}_L + (\bar{\boldsymbol{R}}_L - \boldsymbol{R}_L) {}^L\boldsymbol{b}_1 & \\ \boldsymbol{p}_{R2} = \boldsymbol{p}_L + \boldsymbol{R}_L {}^L\boldsymbol{b}_2 + \left(\frac{\|\bar{\boldsymbol{f}}_2\|}{k_2} + l_{02} \right) \frac{\bar{\boldsymbol{f}}_2}{\|\bar{\boldsymbol{f}}_2\|}. & \end{aligned} \tag{16}$$

We denote with $\mathscr{Q}(t_L, \bar{\boldsymbol{q}}_L)$ *the set of configurations respecting* (16)*.*

Proof. Given $t_L \in \mathbb{R}$, and $\bar{\boldsymbol{\pi}}_A \in \Pi_A(\bar{\boldsymbol{q}}_L)$, a configuration $\boldsymbol{q}$ is an equilibrium if $m(\boldsymbol{q}, \boldsymbol{0}, \bar{\boldsymbol{\pi}}_A, \boldsymbol{0}) = \boldsymbol{0}$. The first six rows are $\boldsymbol{K}_A \boldsymbol{q}_R + \boldsymbol{f} - \bar{\boldsymbol{\pi}}_A = \boldsymbol{0}$. Then, from (7) we have that

$$\boldsymbol{f} = \boldsymbol{K}_A(\bar{\boldsymbol{q}}_R - \boldsymbol{q}_R) + \bar{\boldsymbol{f}}. \tag{17}$$

Multiplying both sides of (17) by $\boldsymbol{G}$ and using (11) we obtain

$$\boldsymbol{G}\boldsymbol{K}_A(\bar{\boldsymbol{q}}_R - \boldsymbol{q}_R) + \boldsymbol{G}\bar{\boldsymbol{f}} = \boldsymbol{g}_L. \tag{18}$$

Then, using $\boldsymbol{K}_{A2} = \boldsymbol{0}$, and the expression of $\bar{\boldsymbol{f}}$ in (9), we get

$$\begin{bmatrix} \boldsymbol{K}_{A1} \boldsymbol{e}_{R1} \\ \boldsymbol{S}({}^L\boldsymbol{b}_1)\boldsymbol{R}_L \boldsymbol{K}_{A1} \boldsymbol{e}_{R1} \end{bmatrix} + \begin{bmatrix} m_L g \boldsymbol{e}_3 \\ 2\boldsymbol{S}({}^L\boldsymbol{b}_2)\boldsymbol{R}_L^T \bar{\boldsymbol{R}}_L \boldsymbol{e}_1 t_L \end{bmatrix} = \begin{bmatrix} m_L g \boldsymbol{e}_3 \\ \boldsymbol{0} \end{bmatrix}, \tag{19}$$

where $\boldsymbol{e}_{Ri} = (\bar{\boldsymbol{p}}_{Ri} - \boldsymbol{p}_{Ri})$. The top row of (19) implies that $\boldsymbol{e}_{R1} = \boldsymbol{0}$, hence $\boldsymbol{p}_{R1} = \bar{\boldsymbol{p}}_{R1}$. Replacing $\boldsymbol{e}_{R1} = \boldsymbol{0}$ in the bottom part of (19) we obtain

$$\begin{aligned} \boldsymbol{S}({}^L\boldsymbol{b}_2)\boldsymbol{R}_L^T \bar{\boldsymbol{R}}_L \boldsymbol{e}_1 t_L = \boldsymbol{0} \Leftrightarrow \;\; & {}^L\boldsymbol{b}_2 \times \boldsymbol{R}_L^T \bar{\boldsymbol{R}}_L \boldsymbol{e}_1 t_L = \boldsymbol{0} \\ \Leftrightarrow \;\; & \boldsymbol{R}_L \boldsymbol{e}_1 \times \bar{\boldsymbol{R}}_L \boldsymbol{e}_1 t_L = \boldsymbol{0}. \end{aligned} \tag{20}$$

Finally we can retrieve the remaining components of the equilibrium configuration, namely $\boldsymbol{p}_L$ and $\boldsymbol{p}_{R2}$, using (1) and the system kinematics. □

Remark 4. If $t_L = 0$ the conditions in (20) hold for all possible load attitudes $\boldsymbol{R}_L \in SO(3)$. This means that the set of equilibria with no internal force, i.e., $\mathscr{Q}(0, \bar{\boldsymbol{q}}_L)$, contains all the $\boldsymbol{R}_L \in SO(3)$ and the $\boldsymbol{q}_R$, $\boldsymbol{p}_L$ are computed from $\boldsymbol{R}_L$ using (16). Figure 4 illustrates some of these equilibria.

For $t_L \neq 0$, it is required that $\boldsymbol{R}_L \boldsymbol{e}_1$ is parallel to $\bar{\boldsymbol{R}}_L \boldsymbol{e}_1$. This can be obtained with $\boldsymbol{R}_L = \boldsymbol{R}_L(k, \phi) = \bar{\boldsymbol{R}}_L \boldsymbol{R}_{\boldsymbol{z}_L}(k\pi) \boldsymbol{R}_{\boldsymbol{x}_L}(\phi)$, where $k = 0, 1$, $\phi \in [0, 2\pi]$, and $\boldsymbol{R}_{\boldsymbol{z}_L}(\cdot)$ and $\boldsymbol{R}_{\boldsymbol{x}_L}(\cdot)$ are the rotations about $\boldsymbol{z}_L$ and $\boldsymbol{x}_L$, respectively. Considering that ${}^L\boldsymbol{b}_1$ is parallel to $\boldsymbol{x}_L$ we have that $\boldsymbol{R}_{\boldsymbol{z}_L}(k\pi) \boldsymbol{R}_{\boldsymbol{x}_L}(\phi) {}^L\boldsymbol{b}_1$ is either equal to ${}^L\boldsymbol{b}_1$ if $k = 0$ or to $-{}^L\boldsymbol{b}_1$

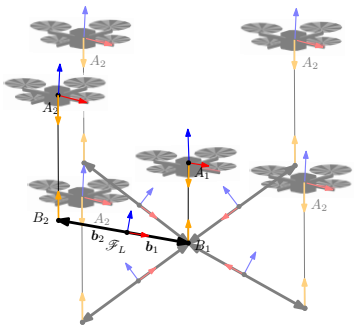

Fig. 4: Five of the infinite possible equilibrium configurations for $t_L = 0$. In vivid color the configuration $\bar{\boldsymbol{q}}$. In opaque color some of the other possible equilibrium configurations in $\mathscr{Q}(0, \bar{\boldsymbol{q}}_L)$.

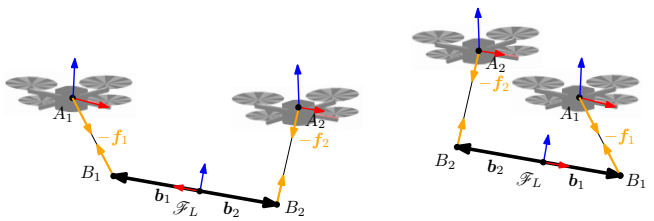

Fig. 5: 2D representation of two equilibria for $t_L \neq 0$. On the left and on the right one equilibrium configuration in $\mathscr{Q}^+(t_L, \bar{\boldsymbol{q}}_L)$ and $\mathscr{Q}^-(t_L, \bar{\boldsymbol{q}}_L)$, respectively.

if $k = 1$. Therefore, using (16), we obtain either $\boldsymbol{p}_L = \bar{\boldsymbol{p}}_L$ if $k = 0$ or $\boldsymbol{p}_L = \bar{\boldsymbol{p}}_L + 2\boldsymbol{b}_1$ if $k = 1$.

Fig. 5 provides a simplified representations of the two different sets of equilibria for $k = 0$ and $k = 1$, formally defined as follows:

- $\mathscr{Q}^+(t_L, \bar{\boldsymbol{q}}_L) = \{\boldsymbol{q} \in \mathscr{Q}(t_L, \bar{\boldsymbol{q}}_L) | \boldsymbol{R}_L = \boldsymbol{R}_L(0, \phi) \forall \phi\}$,
- $\mathscr{Q}^-(t_L, \bar{\boldsymbol{q}}_L) = \{\boldsymbol{q} \in \mathscr{Q}(t_L, \bar{\boldsymbol{q}}_L) | \boldsymbol{R}_L = \boldsymbol{R}_L(1, \phi) \forall \phi\}$.

Notice that $\mathscr{Q}(0, \bar{\boldsymbol{q}}_L)$ is parametrized by an element in $SO(3)$ (any $\boldsymbol{R}_L \in SO(3)$ is allowed), while and $\mathscr{Q}^+(t_L, \bar{\boldsymbol{q}}_L)$, $\mathscr{Q}^-(t_L, \bar{\boldsymbol{q}}_L)$, for $t_L \neq 0$, are parametrized by an element in $SO(1)$ ($\boldsymbol{R}_L(0, \phi)$ and $\boldsymbol{R}_L(1, \phi)$, for any $\phi \in [0, 2\pi[$, respectively). In particular for all cases, the load rotation about $\boldsymbol{x}_L$ can be any. This because the robots can not apply any moment along $\boldsymbol{x}_L$, and the corresponding rotation results uncontrollable. Practically this is not an issue since the orientation of a beam about $\boldsymbol{x}_L$ is usually not of interest and it is anyway passively stabilized by the structure.

At the end of this section we can conclude that choosing $t_L \neq 0$ (equilibrium with vertical cables) is the worse option because any orientation of the load is contained in the equilibrium set for this choice. Furthermore, the load equilibrium positions are free to move on sphere of radius $\|{}^L\boldsymbol{b}_1\|$ centered on B_1. Contrarily, $t_L \neq 0$ is a much better choice, in fact in this case, a part from the rotation about the $\boldsymbol{x}_L$ axis, there are only two distinct equilibria, in one it is exactly $\boldsymbol{q}_L = \bar{\boldsymbol{q}}_L$, as expected, and in the other one the load orientation is parallel to the one in $\bar{\boldsymbol{q}}_L$ but position is reflected w.r.t. B_1.

B. Stability of the Equilibria

In this section we shall analyze the stability of the equilibria discovered in Sec. III-A. Firstly we define $\boldsymbol{x} = (\boldsymbol{q}, \boldsymbol{v})$ as the state of the system, $\bar{\boldsymbol{x}} = (\bar{\boldsymbol{q}}, \boldsymbol{0})$ the desired equilibrium state, and the following sets (subspaces of the state space) that are related to the previous sets of equilibria:

- $\mathscr{X}(t_L, \bar{\boldsymbol{q}}_L) = \{\boldsymbol{x} : \boldsymbol{q} \in \mathscr{Q}(t_L, \bar{\boldsymbol{q}}_L),\ \boldsymbol{v} = \boldsymbol{0}\}$
- $\mathscr{X}(0, \bar{\boldsymbol{q}}_L) = \{\boldsymbol{x} : \boldsymbol{q} \in \mathscr{Q}(0, \bar{\boldsymbol{q}}_L),\ \boldsymbol{v} = \boldsymbol{0}\}$
- $\mathscr{X}^+(t_L, \bar{\boldsymbol{q}}_L) = \{\boldsymbol{x} : \boldsymbol{q} \in \mathscr{Q}^+(t_L, \bar{\boldsymbol{q}}_L),\ \boldsymbol{v} = \boldsymbol{0}\}$
- $\mathscr{X}^-(t_L, \bar{\boldsymbol{q}}_L) = \{\boldsymbol{x} : \boldsymbol{q} \in \mathscr{Q}^-(t_L, \bar{\boldsymbol{q}}_L),\ \boldsymbol{v} = \boldsymbol{0}\}$

Theorem 3. *Let us consider a desired load configuration $\bar{\boldsymbol{q}}_L$ and the autonomous system* (4) *and let the constant forcing input $\boldsymbol{\pi}_A$ be chosen in $\Pi_A(\bar{\boldsymbol{q}}_L)$ corresponding to a certain internal force t_L, then the following holds:*

- $t_L > 0 \Rightarrow \mathscr{X}^+(t_L, \bar{\boldsymbol{q}}_L)$ *is locally asymptotically stable;*
- $t_L > 0 \Rightarrow \mathscr{X}^-(t_L, \bar{\boldsymbol{q}}_L)$ *is unstable;*
- $\mathscr{X}(0, \bar{\boldsymbol{q}}_L)$ *is locally asymptotically stable;*
- $t_L < 0 \Rightarrow \mathscr{X}^+(t_L, \bar{\boldsymbol{q}}_L)$ *is unstable;*
- $t_L < 0 \Rightarrow \mathscr{X}^-(t_L, \bar{\boldsymbol{q}}_L)$ *is locally asymptotically stable.*

Proof. Let us consider the following Lyapunov candidate:

$$\begin{aligned} V(\boldsymbol{x}) = &\frac{1}{2}(\boldsymbol{v}_R^T \boldsymbol{M}_A \boldsymbol{v}_R + \boldsymbol{e}_R^T \boldsymbol{K}_A \boldsymbol{e}_R + \boldsymbol{v}_L^T \boldsymbol{M}_L \boldsymbol{v}_L + \\ &+ k_1(\|\boldsymbol{l}_1\| - l_{01})^2 - \boldsymbol{l}_1^T \bar{\boldsymbol{f}}_1 + k_2(\|\boldsymbol{l}_2\| - l_{02})^2) + \\ &- \boldsymbol{l}_2^T \bar{\boldsymbol{f}}_2 + t_L(1 - (\bar{\boldsymbol{R}}_L \boldsymbol{e}_1)^T \boldsymbol{R}_L \boldsymbol{e}_1) + V_0, \end{aligned} \tag{21}$$

where $V_0 \in \mathbb{R}_{\geq 0}$. $V(\boldsymbol{x})$ is a lower bounded, continuously differentiable function in the domain of interest. In order to see that $V(\boldsymbol{x})$ is lower bounded it is sufficient to show that the terms $k_i(\|\boldsymbol{l}_i\| - l_{0i})^2 - \boldsymbol{l}_i^T \bar{\boldsymbol{f}}_i$, for $i = 1, 2$, are lower bounded, since all the others are clearly lower bounded. This can be demonstrated by defining $\boldsymbol{a} = 2\bar{\boldsymbol{f}}_i / k_i$ and observing that :

$$\begin{aligned} (\|\boldsymbol{l}_i\| - l_{0i})^2 - \boldsymbol{a}^T \boldsymbol{l}_i &= \|\boldsymbol{l}_i\|^2 - 2\|\boldsymbol{l}_i\| l_{0i} + l_{0i}^2 - \boldsymbol{a}^T \boldsymbol{l}_i \\ &\geq \|\boldsymbol{l}_i\|^2 - 2\|\boldsymbol{l}_i\| l_{0i} - \|\boldsymbol{a}\| \|\boldsymbol{l}_i\| \\ &\geq \|\boldsymbol{l}_i\|^2 - (2l_{0i} - \|\boldsymbol{a}\|)\|\boldsymbol{l}_i\|. \end{aligned}$$

Therefore (21) is lower bounded. If $t_L \geq 0$, then we can choose the term V_0 such that $V(\boldsymbol{x}) \geq 0$ and $V(\bar{\boldsymbol{x}}) = 0$. Notice that $V(\boldsymbol{x})$ is only positive semi definite. Indeed, $V(\boldsymbol{x}) = 0$ for all $\boldsymbol{x} \in \mathscr{X}(0, \bar{\boldsymbol{q}}_L)$ and $\boldsymbol{x} \in \mathscr{X}^+(t_L, \bar{\boldsymbol{q}}_L)$ with $t_L > 0$.

Let us now compute the time derivative of (21):

$$\begin{aligned} \dot{V}(\boldsymbol{x}) = &\boldsymbol{v}_R^T \boldsymbol{M}_A \dot{\boldsymbol{v}}_R + \boldsymbol{v}_L^T \boldsymbol{M}_L \dot{\boldsymbol{v}}_L + \boldsymbol{e}_R \boldsymbol{K}_A \boldsymbol{v}_R + \\ &+ k_1(\|\boldsymbol{l}_1\| - l_{01}) \frac{\boldsymbol{l}_1^T}{\|\boldsymbol{l}_1\|} \dot{\boldsymbol{l}}_1 + k_2(\|\boldsymbol{l}_2\| - l_{02}) \frac{\boldsymbol{l}_2^T}{\|\boldsymbol{l}_2\|} \dot{\boldsymbol{l}}_2 + \\ &+ \bar{\boldsymbol{f}}_1^T \dot{\boldsymbol{l}}_1 + \bar{\boldsymbol{f}}_2^T \dot{\boldsymbol{l}}_2 - t_L \boldsymbol{e}_1^T \bar{\boldsymbol{R}}_L^T \dot{\bar{\boldsymbol{R}}}_L \boldsymbol{e}_1. \end{aligned} \tag{22}$$

Replacing (4), (1) and (9) in (22) we obtain

$$\begin{aligned} \dot{V} = &\boldsymbol{v}_R^T \boldsymbol{M}_A \dot{\boldsymbol{v}}_R + \boldsymbol{v}_L^T \boldsymbol{M}_L \dot{\boldsymbol{v}}_L + \boldsymbol{e}_R \boldsymbol{K}_A \boldsymbol{v}_R + \\ &+ (\boldsymbol{f}_1 - t_L \bar{\boldsymbol{R}}_L \boldsymbol{e}_1 - m_L g \boldsymbol{e}_3/2)^T (\dot{\boldsymbol{p}}_{R1} - \dot{\boldsymbol{p}}_L - \dot{\boldsymbol{R}}_L {}^L\boldsymbol{b}_1) + \\ &+ (\boldsymbol{f}_2 + t_L \bar{\boldsymbol{R}}_L \boldsymbol{e}_1 - m_L g \boldsymbol{e}_3/2)^T (\dot{\boldsymbol{p}}_{R2} - \dot{\boldsymbol{p}}_L - \dot{\boldsymbol{R}}_L {}^L\boldsymbol{b}_2) + \\ &- t_L \boldsymbol{e}_1^T \bar{\boldsymbol{R}}_L^T \dot{\bar{\boldsymbol{R}}}_L \boldsymbol{e}_1 \\ = &-\boldsymbol{v}_R{}^T \boldsymbol{B}_A \boldsymbol{v}_R + \boldsymbol{v}_R{}^T \boldsymbol{u}_A - \boldsymbol{\omega}_L^T \boldsymbol{B}_L \boldsymbol{\omega}_L, \end{aligned} \tag{23}$$

that for $\boldsymbol{u}_A = \boldsymbol{0}$ becomes $\dot{V}(\boldsymbol{x}) = -\boldsymbol{v}_R{}^T \boldsymbol{B}_A \boldsymbol{v}_R - \boldsymbol{\omega}_L^T \boldsymbol{B}_L \boldsymbol{\omega}_L$, that is clearly negative semidefinite. In particular $\dot{V}(\boldsymbol{x}) = 0$ for all $\boldsymbol{x} \in \mathscr{E}\{\boldsymbol{x} : \boldsymbol{v}_R = \boldsymbol{0},\ \boldsymbol{\omega}_L = \boldsymbol{0}\}$

Since $V(\boldsymbol{x})$ is only positive semidefinite, to prove the asymptotic stability we rely on the *LaSalle's invariance principle* [20]. Let us define a positively invariant set $\Omega_\alpha = \{\boldsymbol{x} : V(\boldsymbol{x}) \leq \alpha \text{ with } \alpha \in \mathbb{R}_{>0}\}$. By construction Ω_α is compact since (21) is radially unbounded and Ω_0 is compact ($\Omega_0 = \mathscr{X}(0, \bar{\boldsymbol{q}}_L)$ and $\Omega_0 = \mathscr{X}^+(t_L, \bar{\boldsymbol{q}}_L)$ for $t_L = 0$ and $t_L > 0$, respectively, are both compact sets). Then we need to find the largest invariant set $\mathscr{M}$ in $\mathscr{E} = \{\boldsymbol{x} \in \Omega_\alpha \mid \dot{V}(\boldsymbol{x}) = 0\}$. A trajectory $\boldsymbol{x}(t)$ belongs identically to $\mathscr{E}$ if

$$\dot{V}(\boldsymbol{x}(t)) \equiv 0 \Leftrightarrow \begin{cases} \boldsymbol{v}_R(t) \equiv \boldsymbol{0} \\ \boldsymbol{\omega}_L(t) \equiv \boldsymbol{0} \end{cases} \Leftrightarrow m(\boldsymbol{q}(t), \boldsymbol{0}, \boldsymbol{\pi}_A) = \boldsymbol{0}$$

for all $t \in \mathbb{R}_{>0}$. Therefore $\boldsymbol{x}$ has to be an equilibrium, and for Theorem 2 we have that $\dot{V}(\boldsymbol{x}(t)) \equiv 0 \Leftrightarrow \boldsymbol{x}(t) \in \mathscr{X}(t_L, \bar{\boldsymbol{q}}_L)$. Thus we obtain $\mathscr{M} = \Omega_\alpha \cap \mathscr{X}(t_L, \bar{\boldsymbol{q}}_L)$.

For $t_L > 0$, it is easy to see that for a sufficiently small α, $\mathscr{X}^+(t_L, \bar{\boldsymbol{q}}_L) \subseteq \Omega_\alpha$ but $\mathscr{X}^-(t_L, \bar{\boldsymbol{q}}_L) \cap \Omega_\alpha = \varnothing$. This because $V(\boldsymbol{x}) = 0$ for $\boldsymbol{x} \in \mathscr{X}^+(t_L, \bar{\boldsymbol{q}}_L)$, while $V(\boldsymbol{x}) > 0$ for $\boldsymbol{x} \in \mathscr{X}^-(t_L, \bar{\boldsymbol{q}}_L)$. This comes from the fact that in (21), for $\boldsymbol{x} \in \mathscr{X}^-(t_L, \bar{\boldsymbol{q}}_L)$, the term $t_L(1 - (\bar{\boldsymbol{R}}_L \boldsymbol{e}_1)^T \boldsymbol{R}_L \boldsymbol{e}_1) = 2t_L$. Therefore $\mathscr{M} = \mathscr{X}^+(t_L, \bar{\boldsymbol{q}}_L)$. All conditions of LaSalle's principle are satisfied and $\mathscr{X}^+(t_L, \bar{\boldsymbol{q}}_L)$ is locally asymptotically stable.

On the other hand, for $t_L = 0$ we have that $\mathscr{X}(t_L, \bar{\boldsymbol{q}}_L) \subseteq \Omega_\alpha$ for every sufficiently small α. Therefore $\mathscr{M} = \mathscr{X}(t_L, \bar{\boldsymbol{q}}_L)$ and, as before, we can conclude that $\mathscr{X}(t_L, \bar{\boldsymbol{q}}_L)$ is locally asymptotically stable for the LaSalle's invariance principle.

Now, let us investigate the stability for $t_L < 0$. As before, with an opportune choice of V_0, we have that $V(\boldsymbol{x}) = 0$ for $\boldsymbol{x} \in \mathscr{X}^+(t_L, \bar{\boldsymbol{q}}_L)$. However $\mathscr{X}^+(t_L, \bar{\boldsymbol{q}}_L)$ is a set of accumulation for the points where $V(\boldsymbol{x}) < 0$. Indeed, consider $\boldsymbol{v} = \boldsymbol{0}$, $\boldsymbol{p}_{R1} = \bar{\boldsymbol{p}}_{R1}$, $\boldsymbol{R}_L$ such that $(\bar{\boldsymbol{R}}_L \boldsymbol{e}_1)^T \boldsymbol{R}_L \boldsymbol{e}_1 = 1 - \varepsilon$, with $\varepsilon > 0$ arbitrarily small, $\boldsymbol{p}_L$ and $\boldsymbol{p}_{R2}$ as in (16). Under this conditions, we have that $V(\boldsymbol{x}) = t_L(1 - (\bar{\boldsymbol{R}}_L \boldsymbol{e}_1)^T \boldsymbol{R}_L \boldsymbol{e}_1) = t_L \varepsilon < 0$. Then, $\dot{V}(\boldsymbol{x}) < 0$ in a neighborhood of $\mathscr{X}^+(t_L, \bar{\boldsymbol{q}}_L)$. All conditions of *Chetaev's theorem* [20] are satisfied, and we can conclude that $\mathscr{X}^+(t_L, \bar{\boldsymbol{q}}_L)$ is an unstable set.

Finally, to study the stability of $\mathscr{X}^-(t_L, \bar{\boldsymbol{q}}_L)$ for $t_L \neq 0$, one can always find another desired load configuration $\bar{\boldsymbol{q}}'_L$ for which, choosing $t'_L = -t_L$ and the corresponding $\boldsymbol{\pi}'_A \in \Pi_A(\bar{\boldsymbol{q}}'_L)$, we have $\mathscr{X}^+(t'_L, \bar{\boldsymbol{q}}_L) = \mathscr{X}^-(t_L, \bar{\boldsymbol{q}}_L)$. Assuming $t_L > 0$, we have that $t'_L < 0$ and $\mathscr{X}^+(t'_L, \bar{\boldsymbol{q}}_L)$ is unstable. Therefore $\mathscr{X}^-(t_L, \bar{\boldsymbol{q}}_L)$ is unstable too. A similar reasoning can be done to prove that $\mathscr{X}^-(t_L, \bar{\boldsymbol{q}}_L)$ is locally asymptotically stable for $t_L < 0$. □

IV. Numerical Validation

In this section we shall describe the results of several numerical simulations validating the proposed method and all the presented theoretical concepts and results.

We tested the method in a more realistic scenario. Indeed, we replaced the simplified linear robot dynamics of Sec. II, with the proper nonlinear dynamics of a quadrotor-like vehicle together with a geometric position controller. All the system parameters are reported in Tab. I, together with the admittance controller gains for both robots. A smaller apparent inertia of the slave is chosen to make the slave more sensitive to external forces, and thus more reactive.

System Parameters			**Controller Gains**		
	$i=1$	$i=2$		$i=1$	$i=2$
m_{Ri} [Kg]	1.02	0.993	$\boldsymbol{M}_{Ai}$	$3\boldsymbol{I}_3$	$0.5\boldsymbol{I}_3$
$\boldsymbol{J}_{Ri}$ [Kg·m^2]	$0.015\boldsymbol{I}_3$	$0.015\boldsymbol{I}_3$	$\boldsymbol{B}_{Ai}$	$18\boldsymbol{I}_3$	$1.3\boldsymbol{I}_3$
l_{0i} [m]	1	1	$\boldsymbol{K}_{Ai}$	$15\boldsymbol{I}_3$	$\boldsymbol{0}$
k_i [N/m]	20	20	**Desired Load Pose**		
${}^L\boldsymbol{b}_i$ [m]	[0.433 0 0]	[−0.433 0 0]	$\bar{\boldsymbol{p}}_L = [0.3\ 0.3\ 0.2]^T$ [m]		
$m_L = 0.900$ [Kg], $\boldsymbol{J}_{Lx} = 0.112$ [Kg·m^2]			$\bar{\phi} = 0$, $\bar{\theta} = \pi/8$ [rad]		
$\boldsymbol{J}_{Ly} = 5.681$, $\boldsymbol{J}_{Lz} = 5.681$ [Kg·m^2]			$\bar{\psi} = \pi/7$ [rad]		

TABLE I: Parameters used in the simulations.

Let us consider the desired equilibrium $\bar{\boldsymbol{q}} = (\bar{\boldsymbol{p}}_L, \bar{\boldsymbol{R}}_L)$, whose value are in Tab. I, where $(\bar{\phi}, \bar{\theta}, \bar{\psi})$ are the Euler angles that parametrize $\bar{\boldsymbol{R}}_L$. We performed several simulations with $\boldsymbol{\pi}_A \in \Pi_A(\bar{\boldsymbol{q}}_L)$ computed as in (7) for the cases 1) $t_{L1} = 1.5$ [N] > 0, 2) $t_{L2} = 0$ [N], 3) $t_{L3} = -1$ [N] < 0,

We first initialized the system in different initial configurations and we let the system evolve.

1) For $t_L = t_{L1}$, the system always converges to a state belonging to $\mathscr{X}^+(t_L, \bar{\boldsymbol{q}}_L)$, independently from the initial state, validating the asymptotic stability of $\mathscr{X}^+(t_L, \bar{\boldsymbol{q}}_L)$ when $t_L > 0$. In Fig. 6 we show the evolution of the system starting from two different initial state.
2) For t_{L2}, the system final state belongs to $\mathscr{X}(0, \bar{\boldsymbol{q}}_L)$. The final attitude of the load depends on the initial state;
3) For t_{L3}, the system never converges to $\mathscr{X}^+(t_L, \bar{\boldsymbol{q}}_L)$ even initializing it very close. This is due to the instability of $\mathscr{X}^+(t_L, \bar{\boldsymbol{q}}_L)$ when $t_L < 0$.

In another set of simulations the master forcing input is chosen such that the master follows a simple smooth polynomial trajectory from an initial position to $\bar{\boldsymbol{p}}_{R1}$.

For both $t_L = t_{L1}$ and $t_L = t_{L2}$ the system remains stable during the master maneuver, showing only small-amplitude damped oscillations. Once the input becomes constant, the master stops and the system converges to $\bar{\boldsymbol{q}}$ for $t_L = t_{L1}$. For $t_L = t_{L2}$, instead the final load attitude depends on the particular motion of the master, and it is general different from $\bar{\boldsymbol{q}}$.

Plots for cases 2) and 3) and the last dynamic case are not reported here due to space limitation. Some representative simulations however available in the attached video.

V. Conclusions

This work deals with the cooperative transportation of a cable-suspended load performed by two aerial vehicles. The proposed master-slave architecture exploits an admittance controller in order to coordinate the robots in a decentralized fashion but with implicit communication only, using the cable forces. The stability of the static equilibria has been studied highlighting the role played by the internal force. In the future it would be interesting to test the method on a real platform and to extend the theoretical analysis to a more general load.

References

[1] M. Tognon, B. Yüksel, G. Buondonno, and A. Franchi, "Dynamic decentralized control for protocentric aerial manipulators," in *2017 IEEE Int. Conf. on Robotics and Automation*, Singapore, May 2017.

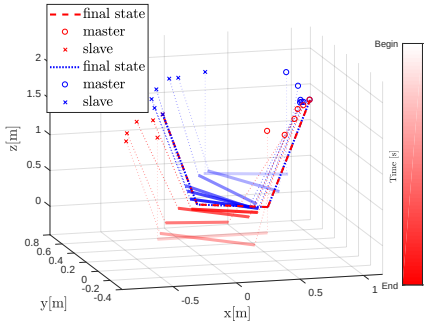

Fig. 6: Evolution of the system for two different initial conditions with $\boldsymbol{\pi}_A \in \Pi_A(\bar{\boldsymbol{q}}_L)$ and $t_L = t_{L1}$. The two evolutions (red and blue, respectively) are represented as sequence of images discriminated by the brightness of the color that represents the time (from bright to dark). The load is represented as a tick solid line, the cables as thin dashed lines, the master robot as a circle and the slave robot as a cross.

[2] M. Tognon and A. Franchi, "Dynamics, control, and estimation for aerial robots tethered by cables or bars," *IEEE Trans. on Robotics*, 2017.

[3] V. Kumar and N. Michael, "Opportunities and challenges with autonomous micro aerial vehicles," *The International Journal of Robotics Research*, vol. 31, no. 11, pp. 1279–1291, 2012.

[4] I. Maza, K. Kondak, M. Bernard, and A. Ollero, "Multi-UAV cooperation and control for load transportation and deployment," *Journal of Intelligent & Robotics Systems*, vol. 57, no. 1-4, pp. 417–449, 2010.

[5] H.-N. Nguyen, S. Park, and D. J. Lee, "Aerial tool operation system using quadrotors as rotating thrust generators," in *2015 IEEE/RSJ Int. Conf. on Intelligent Robots and Systems*, Hamburg, Germany, Oct. 2015, pp. 1285–1291.

[6] R. Ritz and R. D'Andrea, "Carrying a flexible payload with multiple flying vehicles," in *2013 IEEE/RSJ Int. Conf. on Intelligent Robots and Systems*, 2013, pp. 3465–3471.

[7] K. Baizid, F. Caccavale, S. Chiaverini, G. Giglio, and F. Pierri, "Safety in coordinated control of multiple unmanned aerial vehicle manipulator systems: Case of obstacle avoidance," in *2014 22nd Mediterranean Conference of Control and Automation*, 2014, pp. 1299–1304.

[8] H. Y. D. and Lee, "Hierarchical cooperative control framework of multiple quadrotor-manipulator systems," in *2015 IEEE Int. Conf. on Robotics and Automation*, 2015, pp. 4656–4662.

[9] F. Caccavale, G. Giglio, G. Muscio, and F. Pierri, "Cooperative impedance control for multiple uavs with a robotic arm," in *2015 IEEE/RSJ Int. Conf. on Intelligent Robots and Systems*, 2015, pp. 2366–2371.

[10] K. Sreenath and V. Kumar, "Dynamics, control and planning for cooperative manipulation of payloads suspended by cables from multiple quadrotor robots," in *Robotics: Science and Systems*, Berlin, Germany, June 2013.

[11] C. Masone, H. H. Bülthoff, and P. Stegagno, "Cooperative transportation of a payload using quadrotors: A reconfigurable cable-driven parallel robot," in *2016 IEEE/RSJ Int. Conf. on Intelligent Robots and Systems*, Oct 2016, pp. 1623–1630.

[12] N. Michael, J. Fink, and V. Kumar, "Cooperative manipulation and transportation with aerial robots," *Autonomous Robots*, vol. 30, no. 1, pp. 73–86, 2011.

[13] G. Wu and K. Sreenath, "Geometric control of multiple quadrotors transporting a rigid-body load," in *53rd IEEE Conf. on Decision and Control*, 2014, pp. 6141–6148.

[14] D. Mellinger, M. Shomin, N. Michael, and V.Kumar, "Cooperative grasping and transport using multiple quadrotors," in *Int. Symp. on Distributed Autonomous Robotic Systems*, 2013, pp. 545–558.

[15] G. Gioioso, A. Franchi, G. Salvietti, S. Scheggi, and D. Prattichizzo, "The Flying Hand: a formation of UAVs for cooperative aerial telemanipulation," in *2014 IEEE Int. Conf. on Robotics and Automation*, Hong Kong, China, May. 2014, pp. 4335–4341.

[16] Z. Wang and M. Schwager, "Force-amplifying n-robot transport system (force-ants) for cooperative planar manipulation without communication," *The International Journal of Robotics Research*, vol. 35, no. 13, pp. 1564–1586, 2016.

[17] A. Tagliabue, M. Kamel, S. Verling, R. Siegwart, and J. Nieto, "Collaborative object transportation using mavs via passive force control," *arXiv preprint arXiv:1612.04915*, 2016.

[18] M. Gassner, T. Cieslewski, and D. Scaramuzza, "Dynamic collaboration without communication: Vision-based cable-suspended load transport with two quadrotors," in *2017 IEEE Int. Conf. on Robotics and Automation*, Singapore, 2017.

[19] M. Ryll, G. Muscio, F. Pierri, E. Cataldi, G. Antonelli, F. Caccavale, and A. Franchi, "6D physical interaction with a fully actuated aerial robot," in *2017 IEEE Int. Conf. on Robotics and Automation*, Singapore, May 2017.

[20] H. K. Khalil, *Noninear Systems*. Prentice-Hall, New Jersey, 1996.